JOURNAL OF MATERIALS SCIENCE 27 (1992) 4805–4812

Corrosion characteristics of aluminium alloy graphite particulate composite in various environments

M. SAXENA, B. K. PRASAD, T. K. DAN*
Regional Research Laboratory, Council of Scientific and Industrial Research, Hoshangabad Road, Near Habibganj Naka, Bhopal 462 026, India

The present study was aimed at understanding the response of 2014 Al alloy dispersed with graphite particles in various corrosive environments. Marine (sodium chloride) as well as acidic media were selected for the purpose with a view to widen the range of utility of the composite for applications where such environments may be encountered. Studies were also extended to characterize the corrosion resistance of the composite in fresh as well as used lubricating oils to explore the possibilities of using it in bearing, bushing and such other applications. The corrosion behaviour of the base alloy processed under identical conditions was also examined in the above media to see the influence of graphite addition in the alloy. In order to assess the role of the matrix microstructure, the composite as well as the base alloy was subjected to corrosion in heat-treated as well as-cast conditions. It was observed that the specimens suffered from the maximum rate of corrosion in acid, while sodium chloride produced the minimum corrosion rate. Oil in both used and fresh conditions revealed a negligibly small extent of corrosion. The composite was found to show a higher rate of corrosion than the base alloy under identical test conditions. This was attributed to the dispersoid/matrix interfacial corrosion in the case of the graphitic aluminium alloy. Heat treatment of the composite and the base alloy was found to lower the rate of corrosion in the environments tested. Microstructural modifications of the matrix and possible relief of residual stresses were thought to be responsible for the lower rate of corrosion in the heat-treated condition.

1. Introduction

Aluminium alloys dispersed with graphite particles are known as potential materials for tribological applications such as bearings, bushings, pistons, etc., because they offer good resistance to seizure and wear [1, 2]. Their light weight, good fabricability and many other beneficial properties also may make them suitable for structural applications where low strength is required. Aluminium alloys reinforced with graphite fibres are emerging as potential structural materials for aerospace needs and their outstanding mechanical properties have drawn considerable scientific attention to the exploration of their possible applicability to high-technology naval applications [3, 4].

Corrosion characterization of the composites in environments expected to be encountered in service conditions is one of the most important aspects which helps to select a proper material for the purpose. However, due to preoccupation with other problems, corrosion of aluminium alloy-graphite composites has received relatively little attention [3–10] despite its importance for the viability of the product [11].

There are conflicting reports on the corrosion behaviour of aluminium alloy matrix composites. For example, the considerably higher corrosion rate of graphitic aluminium composite compared to the base aluminium–silicon alloy, has been reported by Saxena *et al.* [12], while the corrosion rate of graphitic aluminium alloys was found to be comparable to that of the respective base alloy [5, 7, 13]. The corrosive environment in these studies was an NaCl solution of identical concentrations [5, 7, 12, 13].

It has been observed that there are a number of variables, such as the type of matrix alloy, matrix microstructure, its spatial distribution, dispersoid, nature of the dispersoid/matrix interface, method of fabrication of the composite, environment, etc., which can affect the corrosion resistance of the material and a minor change in any of them would drastically affect its corrosion response [6, 11, 14–16].

The above observations indicate that no standard measure exists which can ensure the corrosion characteristics of aluminium–matrix composites and hence, before putting these into service, examination of their corrosion behaviour becomes important. In this connection, attention has so far been paid towards carrying out corrosion characterization of the composites in different environments. Generally, sea-water

* *Present address*: Extension Centre, CGCRI, Naroda, Ahmedabad 382 330, India.

0022–2461

(NaCl) and lubricating oil have been selected as the environments for studying the corrosion characteristics of the composites [8, 9, 12, 16]. Acids have also been used as the corrosive medium to determine the response of aluminium alloys used for structural applications [17–19]. These environments are encountered by the aluminium alloys used by the chemical and food industries [20, 21]. However, the influence of the dispersion of graphite in the alloys on their corrosion behaviour in acids has not been examined. Information on the effects of matrix microstructure on corrosion properties of aluminium–matrix composites is not available.

In view of this, an attempt has been made to understand the corrosion response of 2014 alloy dispersed with graphite particles in various environments such as marine (NaCl), acidic (hydrochloric, nitric, sulphuric, perchloric acids) and oil. Marine and acidic environments were selected with a view to widen the range of the possible applications of the composites, such as containers, structural components, etc., where such environments may be encountered. Fresh as well as used engine oils were selected for the corrosion studies, bearing in mind the possible uses of the composites in bushing, bearing and such other applications. The base alloy processed under identical conditions was also examined in all the environments to ascertain the influence of graphite addition. The effect of changing matrix microstructure brought about by T6 heat treatment (solution treatment followed by artificial ageing) on the corrosion response of the alloy and the composite was also studied in these environments.

2. Experimental procedure

2.1. Composite preparation

The graphitic aluminium composite was synthesized by the liquid metallurgy route. Heat-treated uncoated graphite particles (size 63–120 μm) were dispersed on the vortex of Alcoa 2014 Al (Al–4.0Cu–0.78Si–0.27Fe–0.62Mn–0.46Mg) alloy melt. A mechanical stirrer was used to create the vortex. The composite melt was solidified in cast iron moulds in the form of cylindrical bars (diameter 20 mm, length 150 mm). The base alloy melt was also cast under identical conditions.

2.2. Heat treatment

Small specimens (diameter 20 mm, length 10 mm) were cut from the cast bars, solution treated at 500 °C for 8 h, quenched in water at 40 °C and aged at 175 °C for 8 h.

2.3. Specimen preparation

Disc-type specimens (diameter 15 mm, thickness 5 mm) were prepared from the composite and the base alloy in heat treated as well as-cast conditions for corrosion testing. The specimens were polished according to standard metallographic techniques. The specimens subjected to tafel and impedance studies were etched with Keller's reagent after polishing.

2.4. Corrosion studies

The corrosion behaviour of the heat treated and cast specimens (alloy and composite) was studied by immersion test and tafel and impedance methods.

2.4.1. Immersion test

A range of environments, e.g. acidic, marine and oil were selected for carrying out immersion tests. They included 0.1 N solution of hydrochloric acid, 3% NaCl and SAE 30 grade lubricating (used and fresh) oil. Weighed specimens of measured dimensions were immersed in the environments and taken out after different test intervals. The tested specimens were then cleaned, dried and weighed. The method adopted for cleaning the specimens corroded in NaCl and acid was as per ASTM standard STP 534 [22]. After oil immersion the specimens were cleaned with xylene. Corrosion rates were computed from weight change measurements.

2.4.2. Tafel and impedance studies

Environments selected for tafel and impedance studies were 0.1 N solutions of HCl, HNO_3, H_2SO_4, $HClO_4$ acids and 3% NaCl. A total exposure area of 1 cm^2 of the specimens was maintained in each case. A saturated calomel electrode was used as the reference electrode and a graphite rod as the counter electrode. Electrochemical measurements were carried out using an EG and G PAR, USA, model 378-1 electrochemical system. The tafel experiments were carried out in the potential range -250 to $+250$ mV at a scanning rate of 1.0 $mV\,s^{-1}$. Impedance measurements were made using a lock-in amplifier in the frequency range 5–10^5 Hz using a sinusoidal a.c. signal of 5 mV. In the fast Fourier transform (FFT) technique, sinusoidal signal of 5 mV amplitude was also used. A merged Nyquist impedance plot was obtained with the help of the FFT and lock-in techniques, and the imaginary component of the impedance, Z'', was plotted against the real component, Z'. From the semicircle obtained, the value of the polarization resistance, R_p, was evaluated. The Stern–Geary [23] equation was used to calculate the value of the corrosion current.

2.5. Microscopy

Metallographically polished and etched (with Keller's reagent) specimens were examined using optical and scanning electron microscopes. Corroded surfaces were examined in an optical microscope. After corrosion tests, sections of the specimens were cut perpendicular to the corroded surfaces, cold mounted in polyester resins, polished according to standard metallographic techniques and etched with Keller's reagent. The transverse sections were observed in the SEM, after sputtering with gold.

3. Results

Fig. 1 shows micrographs of the graphitic 2014 alloy in as-cast and heat-treated conditions. The as-cast matrix structure delineates the dendrites of α-aluminium and the α-$CuAl_2$ eutectic in the interdendritic regions (Fig. 1a). The heat treatment resulted in the spheroidization of $CuAl_2$ precipitate in the matrix.

Fig. 2 reveals the weight change of the alloy and the composite in the as-cast and heat-treated conditions in various environments with the duration of exposure. While dispersion of graphite particles in the matrix increased the corrosion loss, heat treatment reduced the extent of corrosion in NaCl and HCl (Fig. 2a and b). The weight loss in all specimens except the as-cast composite were noted to increase slowly in the initial stage (Stage I), followed by a sudden increase in material loss with exposure time (Stage II) and finally a reduced extent of material loss (Stage III) beyond Stage II in NaCl (Fig. 2a). On the other hand, Stages II and III only were observed in the as-cast composite in the environment (NaCl) as shown in Fig. 2a. The specimens revealed their weight-loss behaviour in HCl (Fig. 2b) to be identical to that of the as-cast composite in NaCl.

A weight gain in the range 0–0.45 mg cm^{-2} (Table I) was observed for the whole span of exposure times, when the specimens were dipped in used as well as fresh oil. Because no definite influence of the dispersion of the graphite or heat treatment could be observed in the case of immersion in oil, the data points have been reported as a band (Fig. 2c). However, the weight gain in general first decreased with exposure time, attained a minimum and then increased further as shown in the figure.

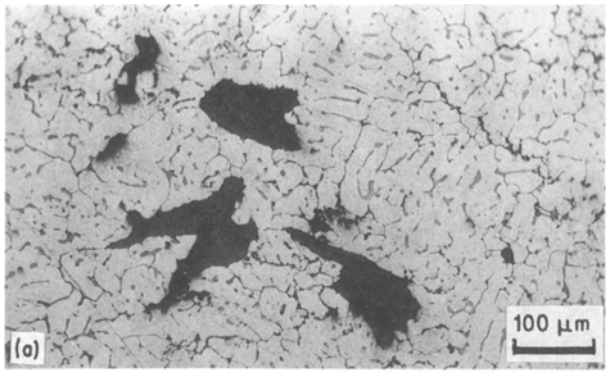

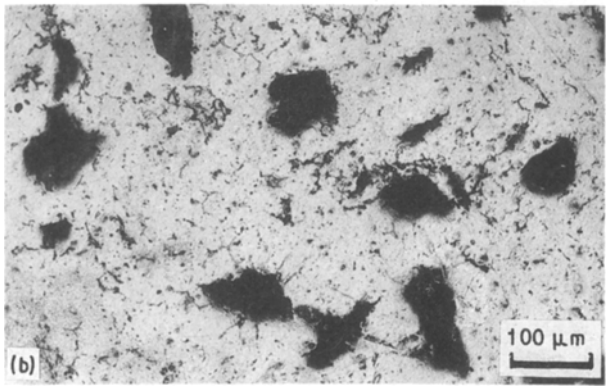

Figure 1 Micrographs of the graphitic 2014 alloy in (a) cast and (b) heat-treated conditions.

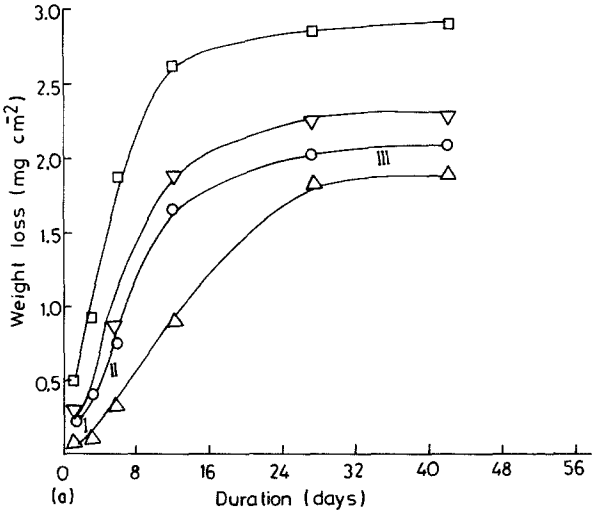

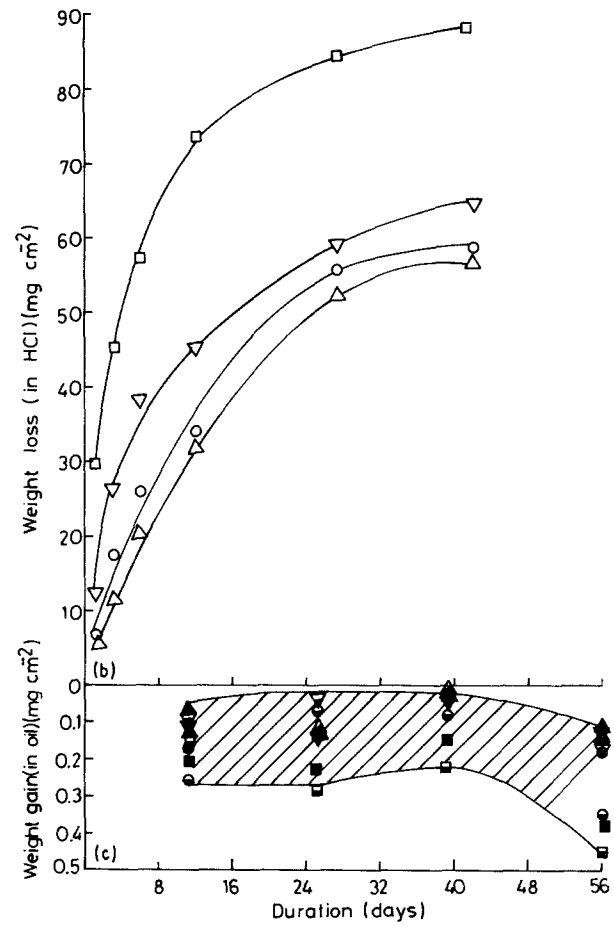

Figure 2 Weight change of the as-cast and heat-treated alloy and composites with the duration of exposure in (a) NaCl (b) HCl and (c) used and fresh oil. NaCl: (○) as-cast 2014, (△) heat-treated 2014, (□) as-cast composite, (▽) heat-treated composite. HCl: (○) as-cast 2014, (△) heat-treated 2014, (□) as-cast composite, (▽) heat-treated composite. Used oil: (◒) as-cast 2014, (▲) heat-treated 2014, (◘) as-cast composite, (▼) heat-treated composite. Fresh oil: (●) as-cast 2014, (▲) heat-treated 2014, (■) as-cast composite, (▼) heat-treated composite.

The corrosion rate, mdd, computed from the weight-loss measurements (Fig. 2) as a function of exposure duration in the immersion test is shown in Fig. 3. The trend observed in all the cases was identical to the weight-loss measurements.

Fig. 4 represents typical tafel plots for the as-cast and heat-treated alloy and composite in HCl. Impedance plots for the specimens in the same environment

TABLE I Corrosion data of as-cast and heat-treated alloy and composite with exposure time in SAE 30 oil

Materials under study	Time of exposure	Used oil			Fresh oil		
		mg cm^{-2}	mdd[a]	mpy[b]	mg cm^{-2}	mdd	mpy
2014	11	+ 0.26	2.38	1.26	0.16	1.51	0.8
as-cast	25	+ 0.07	0.28	0.14	0.13	0.53	0.28
	39	+ 0.08	0.20	0.10	0.02	0.04	0.02
	56	+ 0.35	0.62	0.33	0.18	0.33	0.18
2014	11	+ 0.12	1.04	0.55	0.09	0.88	0.46
HT	25	+ 0.12	0.41	0.22	0.15	0.58	0.30
	39	0	0	0	0.03	0	0
	56	+ 0.12	0.20	0.10	0.13	0.22	0.11
2014	11	+ 0.14	1.29	0.69	0.21	1.96	1.04
comp-cast	25	+ 0.28	1.14	0.60	0.24	0.98	0.52
	39	+ 0.22	0.55	0.29	0.16	0.39	0.21
	56	+ 0.45	0.80	0.42	0.37	0.59	0.31
2014	11	+ 0.09	0.86	0.44	0.11	1.03	0.55
comp-HT	25	+ 0.04	0.16	0.08	0.14	0.58	0.31
	39	+ 0.04	0.11	0.06	0.04	0.10	0.05
	56	+ 0.15	0.26	0.14	0.14	0.25	0.13

[a] mdd = mg dm^{-2} day^{-1}.
[b] mpy = mils penetration $year^{-1}$.

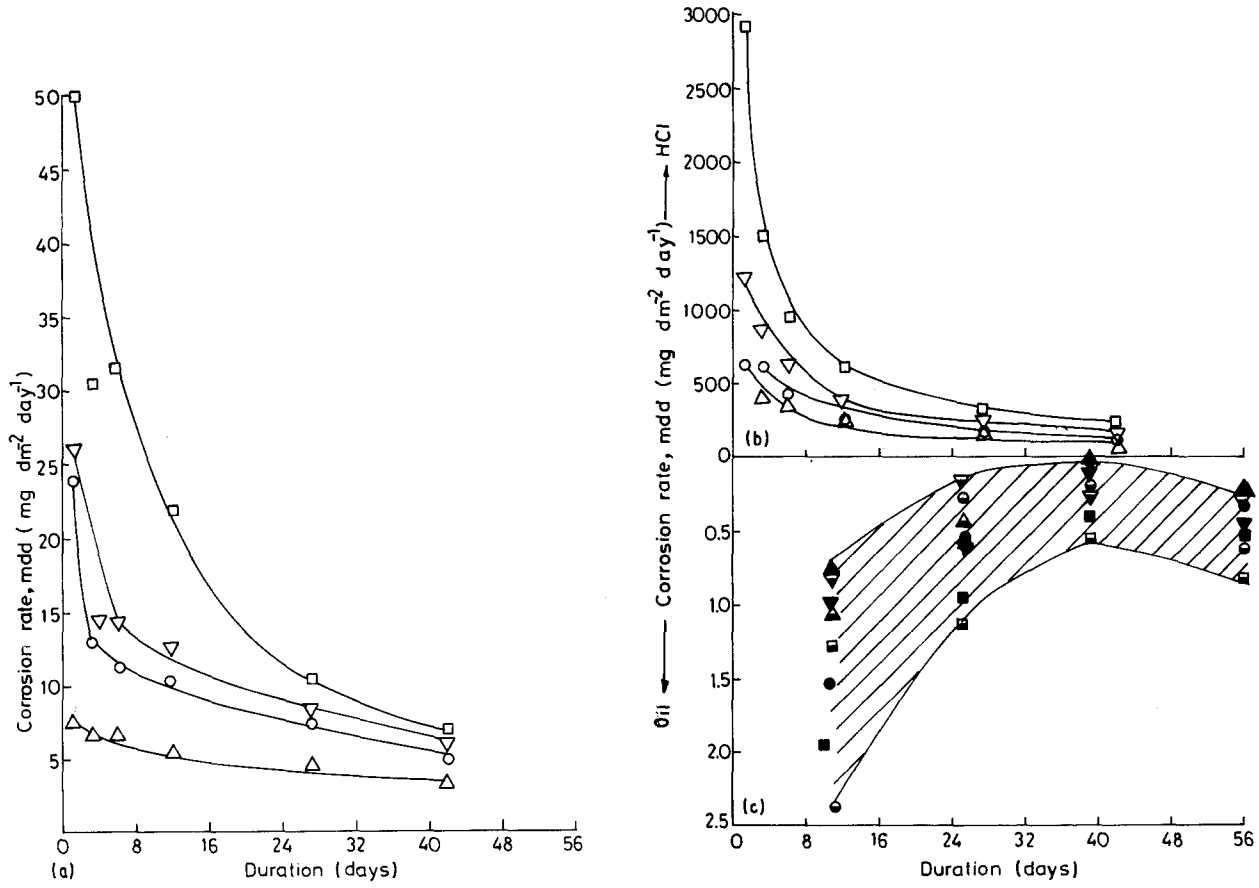

Figure 3 Corrosion rate, mdd, of the specimens, computed from the weight change data of Fig. 2 with exposure time in (a) NaCl, (b) HCl and (c) oil. For key, see Fig. 2.

are shown in Fig. 5. The values of i_{corr} measured by both techniques have been found to be in good agreement with each other for all the specimens (Table II). The behaviour of the specimens in other environments such as HNO_3, H_2SO_4, $HClO_4$ and NaCl, was similar as is evident from the computed values of i_{corr} (Table II). From the severity point of view, the effectiveness of various environments was in the following order: NaCl < $HClO_4$ < H_2SO_4 < HNO_3 < HCl.

The addition of graphite in the matrix increased i_{corr} values in all the environments (Table II) indicating a higher rate of corrosion in the case of the graphitic

TABLE II Corrosion current, i_{corr}, values evaluated by tafel and impedance techniques

Environments under study	Materials	Tafel, i_{corr} ($\mu A\ cm^{-2}$)	Impedance, i_{corr} ($\mu A\ cm^{-2}$)
HCl (0.1 N)	2014 cast	45	41
	2014 HT	31	36
	2014 comp-cast	54	74
	2014 comp-HT	44	45
HNO_3 (0.1 N)	2014 cast	37	29
	2014 HT	22	23
	2014 comp-cast	53	54
	2014 comp-HT	24	29
H_2SO_4 (0.1 N)	2014 cast	32	28
	2014 HT	18	14
	2014 comp-cast	53	53
	2014 comp-HT	25	18
$HClO_4$ (0.1 N)	2014 cast	17	18
	2014 HT	8	8
	2014 comp-cast	28	25
	2014 comp-HT	13	9
NaCl (3%)	2014 cast	3	6
	2014 HT	1	1
	2014 comp-cast	5	4
	2014 comp-HT	3	5

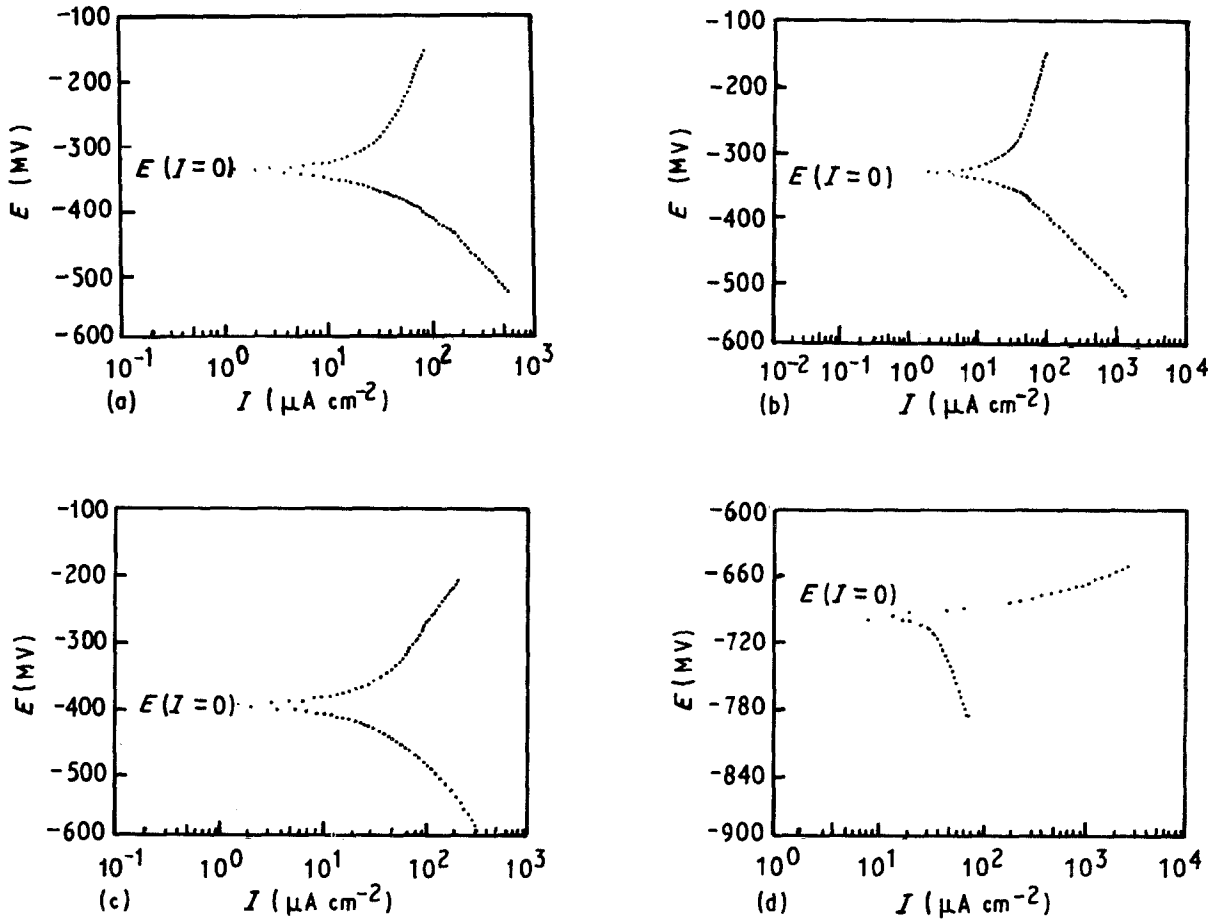

Figure 4 Typical tafel plots of as-cast and heat-treated alloy with and without the dispersion of graphite in HCl. (a) 2014-cast, (b) 2014 HT, (c) 2014 composite cast, (d) 2014 composite HT.

aluminium alloy. Heat treatment was, however, observed to reduce i_{corr}, which indicated a lower corrosion rate of the heat-treated specimens as shown in the table.

Fig. 6 shows the corroded and uncorroded surfaces of the base alloy and the composite in as-cast and heat-treated conditions. Particle/matrix and the precipitate/matrix interfaces were found to have been attacked by the environments in general (Fig. 6a and b, marked A and B, respectively). α-Al was also attacked to some extent as shown in Fig. 6a and b. Corrosive attack on the precipitate/matrix interface

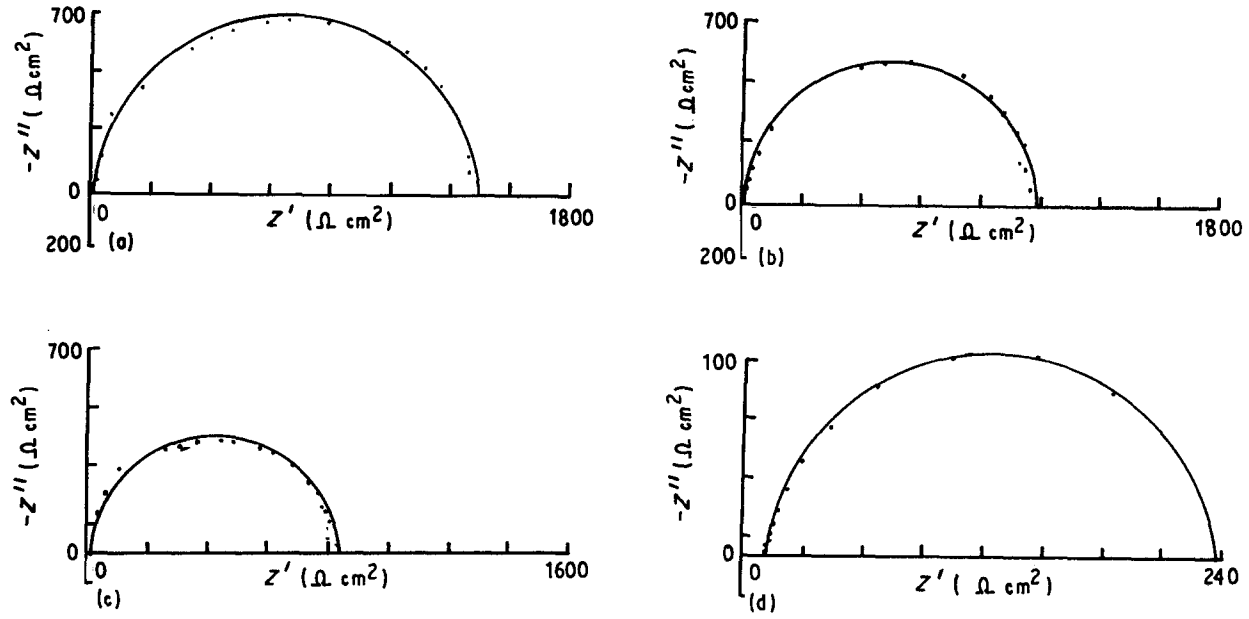

Figure 5 Typical impedance plots of as-cast and heat-treated alloy with and without the dispersion of graphite in HCl. (a) 2014 cast, (b) 2014 HT, (c) 2014 composite cast, (d) 2014 composite HT.

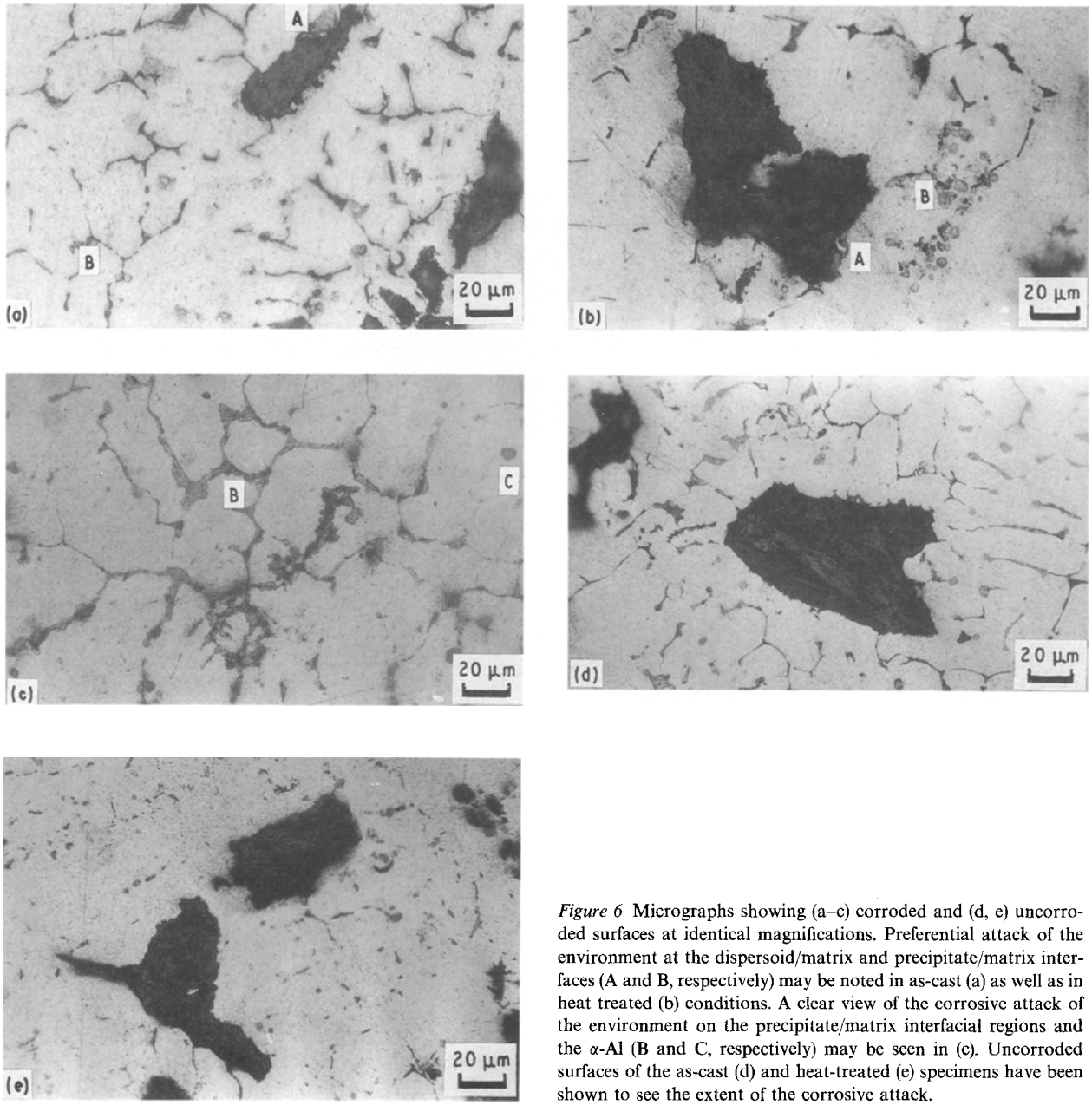

Figure 6 Micrographs showing (a–c) corroded and (d, e) uncorroded surfaces at identical magnifications. Preferential attack of the environment at the dispersoid/matrix and precipitate/matrix interfaces (A and B, respectively) may be noted in as-cast (a) as well as in heat treated (b) conditions. A clear view of the corrosive attack of the environment on the precipitate/matrix interfacial regions and the α-Al (B and C, respectively) may be seen in (c). Uncorroded surfaces of the as-cast (d) and heat-treated (e) specimens have been shown to see the extent of the corrosive attack.

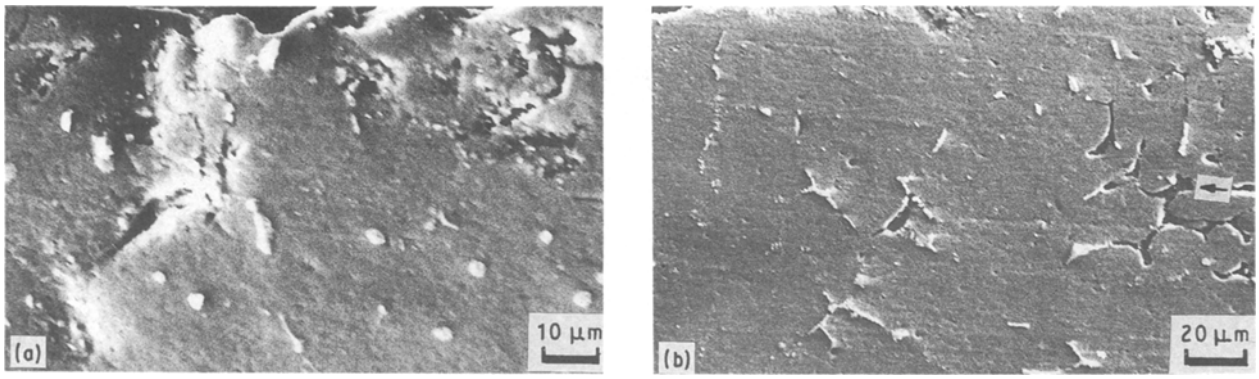

Figure 7 Typical transverse sections of the corroded surfaces of the composite showing (a) the formation of a crater on the surface (top) and (b) $CuAl_2$ precipitate having been eaten away by the corrosive medium (arrowed).

and α-Al may clearly be seen in Fig. 6c (marked B and C, respectively). The micrographs (Fig. 6d and e) of the uncorroded as-cast and heat-treated composites are shown for comparison at identical magnification. Typical micrographs of transverse sections of the corroded surface of the composites are shown in Fig. 7a and b. Formation of craters in the subsurface regions (Fig. 7a) and corrosion of the precipitate/matrix interfacial regions (Fig. 7b) may be noted. In some regions (Fig. 7b, arrowed), the precipitate appears to have been totally eaten away by the environment.

4. Discussion

The mechanism of corrosion in neutral (NaCl) environment involves the formation of stable $Al(OH)_3$ film [24, 25] according to the reaction [26]

$$Al + 3H_2O \rightarrow Al(OH)_3 + 3H^+ + 3e^- \quad (1)$$

The formation of an intermediate species, pseudo boemite (AlOOH), has also been reported elsewhere [25, 27, 28]. This product is finally converted to $Al(OH)_3$ in due course [24, 25]. The latter passivates the surface and retards the rate of further corrosion of the specimen.

On the other hand, in acidic environment corrosion proceeds according to the reaction [26]

$$Al \rightarrow Al^{3+} + 3e^- \quad (2)$$

Here no formation of any stable film takes place and removal proceeds due to continuous dissolution of the specimen surface. After some time, accumulation of the corrosion products on the specimen surface takes place, leading to a reduction in corrosion rate beyond this period.

The slower rate of material loss in the initial stage (Stage I) in NaCl in the case of as-cast alloy and the heat-treated specimens (Fig. 2a) could be attributed to the incubation period [29]. Such an incubation period results from the presence of Al_2O_3 film on the surface which acts as a barrier against the penetration of the corrosive environment. When this film is attacked by the environment and fully or partially removed, fresh surface is exposed to the corrosive environment leading to a sudden increase in material loss (Stage II, Fig. 2a). The presence of stress raiser points, such as inclusions or sharp-edged phases, facilitates the breaking and subsequent removal of the oxide film. After accelerated corrosion has taken place for some time (Stage II), the corrosion products become accumulated on the surface [13] and prevent further penetration of the electrolyte. This causes a reduction in the extent of weight loss (Stage III, Fig. 2a). It appears that by the time the first observations were taken in the case of cast composite in NaCl, the Al_2O_3 film had already vanished, hence the absence of an incubation period in this case (Fig. 2a), as also in HCl (Fig. 2b). The presence of the incubation period of the heat-treated composite in NaCl could be attributed to the relief of internal stresses of the matrix as well as morphological modifications of the precipitate from the needle/plate shape in the as-cast condition (Fig. 1a) to the spheroidized ones after heat treatment (Fig. 1b). At the same time, an increased extent of homogenization of the matrix after heat treatment would also help to reduce the extent of corrosion. These factors were also jointly responsible for reduced corrosion loss of the heat-treated specimens over the cast samples (Fig. 2a and b). The higher material loss of the composite compared to the base alloy under identical conditions was due to the wicking action of the electrolyte by the porous graphite [6]. The dispersoid/matrix interface was another favourable site for attack by the solution [12].

Crater formation in the regions very close to the corroded surface (Fig. 7a) could be due to the formation of micropits resulting from the evolution of hydrogen and the subsequent bursting of bubbles of hydrogen. This led to the localized weakening of the metal [30] causing material loss.

The weight gain (0–0.45 mg cm^{-2}) of the specimens in used and fresh oil corresponding to 0–1.26 mpy (Table I) indicated their insignificant corrosion by the environment as suggested by Fontana *et al.* [31]. Similar weight gain has also been reported in graphitic aluminium alloys in oil by earlier investigators [12, 16]. No explanation of this is available in the literature. However, the weight gain is thought to be affected by two factors: (i) penetration/absorption of the oil in the specimens, and (ii) its removal from the surface. It appears that up to a critical duration of

exposure (and hence a critical depth of penetration) following the cleaning process, the relative retention of oil in the specimens decreased. However, beyond the critical depth of penetration, the oil could not be drained out of the specimen to a considerable extent. This may be responsible for the reduction in weight gain up to some duration of exposure followed by an increase beyond the critical duration (Fig. 2c). The severity of the corrosive attack by the various acidic environments studied may be explained in terms of the capacity of the various anions being adsorbed on the surface of the working electrode (material under investigation). This has been found to be in the following order [32]: $ClO_4^- < SO_4^{-2} < NO_3^- < Cl^-$, which is in good agreement with observations made in this study (Table II).

5. Conclusions

1. The corrosion rate exhibited by the specimens in various environments as observed by the immersion test was HCl > NaCl > oil. There was no observable corrosion of the specimens in oil (used and fresh). This was also evinced by a negligible weight gain of the specimen after immersion in oil.

2. In tafel and impedance tests, the corrosion rate of the specimens varied in various environments in the following order: $NaCl < HClO_4 < H_2SO_4 < HNO_3 < HCl$.

3. The higher corrosion rate of the composite than the base alloy in NaCl and acids in all the tests was due to galvanic attack by the environments at the graphite/aluminium interface and the wicking effect of the electrolyte by the dispersoid phase.

4. Heat-treated specimens exhibited a lower corrosion rate in NaCl and acids as observed by the immersion as well as tafel and impedance studies. This was thought to be due to the changed morphology of the phases, such as $CuAl_2$, and the possible relief of internal stresses from and increased extent of homogenization of the matrix caused by heat treatment.

Acknowledgement

The authors thank Professor T. C. Rao, Director, RRL, Bhopal, for his encouragement and granting permission to publish the work.

References

1. V. G. GURBUNOV, V. D. PARSHIN and V. V. PAMIN, *Russ. Cast. Prod.* (1974) 348.
2. N. A. P. RAO, S. BISWAS, P. K. ROHATGI, A. SANTHANAM and K. NARAYANASWAMY, *Tribo. Int.* **13** (1980) 171.
3. D. M. AYLOR, R. J. FERRARA and R. M. KAIN, *Mater. Perform.* **23** (1984) 32.
4. M. G. VASSILAROS, D. A. DAVIS, G. L. STECKER and J. P. GUDAS, in "Proceedings of the Tri-Service Conference on Corrosion", US Air Force, Academy, Colorado, November 1980, Vol. II.
5. A. M. PATTON, *J. Inst. Metals* **100** (1972) 197.
6. D. M. AYLOR and P. J. MORAN, *J. Electrochem. Soc.* **132** (1985) 1277.
7. R. CHANDRASHEKHAR and P. K. ROHATGI, in "Proceedings of the International Symposium on Industrial Electrochemistry", SAEST (1976) p. 15.
8. *Idem. Trans. Ind. Inst. Metals* **31** (1978) 452.
9. B. P. KRISHNAN, N. RAMAN, K. NARAYANASWAMY and P. K. ROHATGI, *Tribo. Int.* **16** (1983) 241.
10. D. A. DAVIS, M. G. VASSILAROS and J. P. GUDAS, *Mater. Perform.* **21** (1982) 38.
11. M. METZGER and S. G. FISHMANN, *Ind. Eng. Chem. Prod. Res. Dev.* **22** (1983) 296.
12. M. SAXENA, O. P. MODI, A. H. YEGNESWARAN and P. K. ROHATGI, *Corros. Sci.* **27** (1987) 249.
13. J. W. EVANS and D. M. BRADDICK, *ibid.* **11** (1971) 671.
14. DEONATH and T. K. G. NAMBOODIRI, *ibid.* **29** (1989) 1215.
15. S. L. POHLMAN, *Corrosion* **34** (1978) 156.
16. P. R. GIBSON, A. J. CLEGG and A. A. DAS, *Mater. Technol.* **1** (1985) 559.
17. E. H. HOLLINGSWORTH and H. Y. HUNSICKER, in "Metals Handbook", 9th Edn, Vol. 2, edited by C. W. Kirkpatrick, H. Backer and D. Benjamin (American Society for Metals, Metals Park, OH, 1979) p. 204.
18. P. L. CABOT, J. A. GAROIDO, E. PEREJ and J. VIRGILI, *Corros. Sci.* **26** (1986) 357.
19. F. OVARI, L. TOMASANYL and T. TURMEZEY, *Electrochim Acta* **33** (1988) 323.
20. "Aluminium in the chemical and food industries" (British Aluminium Company Ltd, 1966).
21. "Aluminium with food and chemicals", 3rd Edn (The Aluminium Association, Washington, 1975).
22. F. H. COCKS, "Manual of Industrial Corrosion Standards and Control", ASTM STP 534 (American Society for Testing and Materials, Philadelphia, PA, 1973) p. 262.
23. M. STERN and A. L. GEARY, *J. Electrochem. Soc.* **102** (1955) 609.
24. J. AUGUSTYNSKI, in "Passivity in Metals", edited by R. P. Frankenthal and J. Kruger (Electrochemical Society, Pennington, NJ, 1978) p. 973.
25. R. S. ALWITT, "Oxides and Oxide Films", Vol. 4 (Marcel Dekker, New York, 1976) p. 169.
26. W. C. MOSHIER, G. D. DAVIS and J. S. AHEARN, *Corros. Sci.* **27** (1987) 785.
27. W. VEDDER and D. A. VERMILYEA, *Trans. Farad. Soc.* **65** (1969) 561.
28. R. K. HART, *ibid.* **53** (1957) 1020.
29. H. H. STREHBLOW, in "International Congress on Metallic Corrosion" (National Research Council, Canada, 1984) p. 99.
30. B. VYAS and C. M. PREECE, "Erosion Wear and Interfaces with corrosion", ASTM STP 567 (American Society for Testing and Materials, Philadelphia, PA, 1974) p. 77.
31. M. G. FONTANA and N. D. GREENE, "Corrosion Engineering", 2nd Edn (McGraw-Hill International, London, 1978) p. 223.
32. L. L. SHREIR, "Corrosion", Vol. 1 (Newnes Butterworths, Boston, 1979) p. 4: 23.

Received 8 May
and accepted 8 October 1991